ACCOUNTS of chemical research

Article

pubs.acs.org/accounts

Nonadiabatic Excited-State Molecular Dynamics: Modeling Photophysics in Organic Conjugated Materials

Tammie Nelson,*[,†] Sebastian Fernandez-Alberti,[‡] Adrian E. Roitberg,[§] and Sergei Tretiak[†]

[†]Los Alamos National Laboratory, Theoretical Division, Los Alamos, New Mexico 87545, United States

[‡]Universidad Nacional de Quilmes, B1876BXD Bernal, Argentina

[§]Quantum Theory Project, Department of Chemistry, University of Florida, Gainesville, Florida 32611, United States

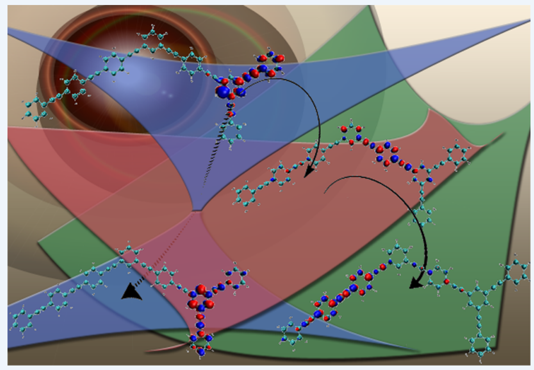

CONSPECTUS: To design functional photoactive materials for a variety of technological applications, researchers need to understand their electronic properties in detail and have ways to control their photoinduced pathways. When excited by photons of light, organic conjugated materials (OCMs) show dynamics that are often characterized by large nonadiabatic (NA) couplings between multiple excited states through a breakdown of the Born−Oppenheimer (BO) approximation. Following photoexcitation, various nonradiative intraband relaxation pathways can lead to a number of complex processes. Therefore, computational simulation of nonadiabatic molecular dynamics is an indispensable tool for understanding complex photoinduced processes such as internal conversion, energy transfer, charge separation, and spatial localization of excitons.

Over the years, we have developed a nonadiabatic excited-state molecular dynamics (NA-ESMD) framework that efficiently and accurately describes photoinduced phenomena in extended conjugated molecular systems. We use the fewest-switches surface hopping (FSSH) algorithm to treat quantum transitions among multiple adiabatic excited state potential energy surfaces (PESs). Extended molecular systems often contain hundreds of atoms and involve large densities of excited states that participate in the photoinduced dynamics. We can achieve an accurate description of the multiple excited states using the configuration interaction single (CIS) formalism with a semiempirical model Hamiltonian. Analytical techniques allow the trajectory to be propagated "on the fly" using the complete set of NA coupling terms and remove computational bottlenecks in the evaluation of excited-state gradients and NA couplings. Furthermore, the use of state-specific gradients for propagation of nuclei on the native excited-state PES eliminates the need for simplifications such as the classical path approximation (CPA), which only uses ground-state gradients. Thus, the NA-ESMD methodology offers a computationally tractable route for simulating hundreds of atoms on ~10 ps time scales where multiple coupled excited states are involved.

In this Account, we review recent developments in the NA-ESMD modeling of photoinduced dynamics in extended conjugated molecules involving multiple coupled electronic states. We have successfully applied the outlined NA-ESMD framework to study ultrafast conformational planarization in polyfluorenes where the rate of torsional relaxation can be controlled based on the initial excitation. With the addition of the state reassignment algorithm to identify instances of unavoided crossings between noninteracting PESs, NA-ESMD can now be used to study systems in which these so-called trivial unavoided crossings are expected to predominate. We employ this technique to analyze the energy transfer between poly(phenylene vinylene) (PPV) segments where conformational fluctuations give rise to numerous instances of unavoided crossings leading to multiple pathways and complex energy transfer dynamics that cannot be described using a simple Förster model. In addition, we have investigated the mechanism of ultrafast unidirectional energy transfer in dendrimers composed of poly(phenylene ethynylene) (PPE) chromophores and have demonstrated that differential nuclear motion favors downhill energy transfer in dendrimers. The use of native excited-state gradients allows us to observe this feature.

1. INTRODUCTION

In recent years, organic conjugated materials (OCMs), such as polymers, small molecules, molecular crystals, and donor−acceptor systems, have emerged as attractive candidates for technological applications.[1−5] Their favorable electronic properties arise from delocalized and highly polarizable π-electrons that support mobile charge carriers.[6] Unlike traditional semiconductors, the excited-state electronic structure of OCMs is complex due to their low dimensionality, strong electronic correlations, and significant electron−phonon coupling.[7] Consequently, the entire evolution of electronic excitations is defined by nonadiabatic (NA) dynamics involving multiple electronic excited states through a breakdown of the Born−Oppenheimer (BO) approximation. Following photoexcitation, intraband relaxation through the manifold of vibrational and electronic excited states can occur leading to energy transfer, excitation localization/delocalization, charge separation, and nonradiative relaxation to the ground or low lying excited states. Understanding and controlling these photoinduced pathways lies at the

Received: October 31, 2013
Published: March 27, 2014

heart of our efforts to design functional photoactive materials. Therefore, it is essential to develop an accurate description of photophysical processes such as exciton formation, evolution, and decay via NA dynamics.[8]

However, sophisticated modeling of nanometer length scales and the sub-nanosecond time scale dynamics of excited electron-vibrational states still poses numerical challenges. Some success has been achieved for the adiabatic or BO molecular dynamics propagating the trajectory along the ground[9] or excited state molecular potential energy surfaces (PESs).[10,11] For example, the semiempirical excited-state molecular dynamics (ESMD) approach allows ultrafast dynamics to be followed on femtosecond to nanosecond time scales in large organic molecules.[7,12,13] The situation becomes more complex when electronic and nuclear dynamics are nonadiabatic. In such cases, straightforward quantum mechanical simulations are not feasible and the description must go beyond the Born−Oppenheimer approximation.[14] Semiclassical methods involving *ab initio* multiple spawning (AIMS)[15] or multiconfigurational time-dependent Hartree (MCTDH)[16] have been developed but are currently limited by computational expense to systems with ∼50−100 degrees of freedom. In particular, MCTDH has been used to study ultrafast exciton dynamics and charge separation in extended conjugated polymers.[17]

Molecular dynamics with quantum transitions (MDQT), particularly the fewest-switches surface hopping (FSSH) approach,[18] is a well-tested method for simulating NA dynamics. The success of FSSH has been previously demonstrated in a wide range of systems.[19−23] The surface hopping approach is illustrated in Figure 1A: following excitation, nuclei evolve along the excited state PES, $E_\alpha(\mathbf{R})$, of the current state. Nuclei are treated classically, while electrons are treated quantum mechanically, and transitions (hops) among coupled excited states incorporate feedback between electronic and nuclear subsystems. At the single trajectory level (Figure1B), detailed insights into mechanistic information can be gained, while observables such as excited-state lifetimes and energy or charge transfer rates are averages over many trajectories. The statistical ensemble of trajectories used in surface hopping algorithms allows quantum yields[24] and branching ratios[25] to be determined quantitatively.

In this Account, we present the nonadiabatic excited-state molecular dynamics (NA-ESMD) methodology developed by our group in recent years.[26−29] NA-ESMD extends the ESMD framework to incorporate quantum transitions using the FSSH scheme. Excited-state calculations are performed using the collective electronic oscillator (CEO) approach[30,31] at the configuration interaction singles (CIS)[32] level combined with the semiempirical AM1[33] model Hamiltonian. This methodology serves as a numerically efficient technique for computing excited states in large conjugated systems and has previously been shown to be adequate for excitonic state description, interstate crossings, and NA dynamics in this class of molecular systems.[34] Analytical excited-state gradients[35−37] and NA couplings[38,39] allow propagation of the trajectory along the native excited-state PES "on the fly". As a result, the NA-ESMD methodology allows simulation of NA dynamics in molecular systems with hundreds of atoms on ∼10 ps time scales. Before running NA-ESMD simulations, it is essential to benchmark the performance of CIS/semiempirical approaches for single-point excited-state calculations against experimental data or more accurate electronic structure techniques (e.g., TDDFT). As we will demonstrate, these simulations have made it possible to successfully model a variety of photoinduced processes in extended molecular systems.

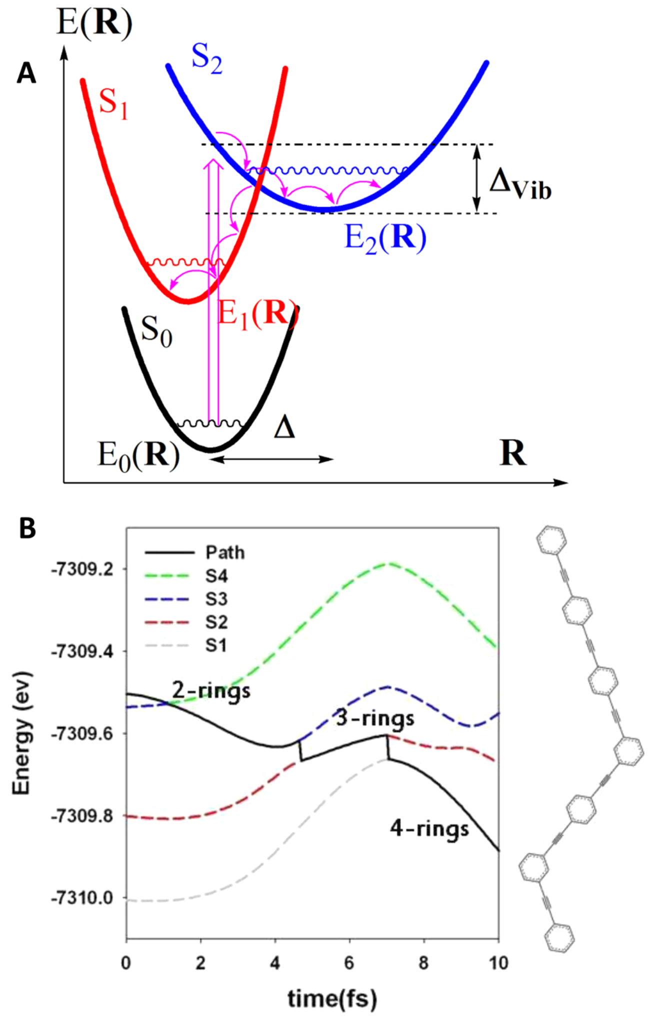

Figure 1. (A) Excited-state energy, $E(\mathbf{R})$, as a function of nuclear coordinates, $\mathbf{R}$. Nuclei evolve on the excited-state BO PES, and transitions between electronic states occur. (B) Representative trajectory showing the path followed after photoexcitation of a poly(phenylene ethynylene) dendrimer.

2. NA-ESMD METHODOLOGY

In this section, we describe details for practical implementation of NA-ESMD. The NA-ESMD algorithm is shown schematically in Scheme 1 and briefly explained herein.

2.1. FSSH Principle

The total time-dependent electronic wave function is a mixed state, expanded in terms of adiabatic basis functions[18]

$$\Psi(\mathbf{r}, \mathbf{R}, t) = \sum_\alpha c_\alpha(t)\phi_\alpha(\mathbf{r}; \mathbf{R}(t)) \tag{1}$$

where $\mathbf{r}$ and $\mathbf{R}$ are electronic and nuclear coordinates, respectively, and $c_\alpha(t)$ are time-dependent expansion coefficients. The equation of motion for $c_\alpha(t)$ simplifies in the adiabatic Hamiltonian eigenstates, ϕ_α, as[18]

$$i\hbar\dot{c}_\alpha(t) = c_\alpha(t)E_\alpha(\mathbf{R}) - i\hbar\sum_\beta c_\beta(t)\dot{\mathbf{R}}\cdot\mathbf{d}_{\alpha\beta} \tag{2}$$

where $\mathbf{d}_{\alpha\beta} = \langle\phi_\alpha(\mathbf{r};\ \mathrm{R})|\nabla_{\mathrm{R}}\phi_\beta(\mathbf{r};\ \mathbf{R})\rangle$ is the NA coupling vector (NACR) and the scalar NA coupling term (NACT) is $\dot{\mathbf{R}}\cdot\mathbf{d}_{\alpha\beta} = \langle\phi_\alpha(\mathbf{r};\ \mathbf{R})|(\partial\phi_\beta(\mathbf{r};\ \mathbf{R}))/(\partial t)\rangle$.[18,40] The time-dependent elements of the density matrix are $a_{\alpha\beta}(t) = c_\alpha^*(t)c_\beta(t)$, where

Scheme 1. NA-ESMD Algorithm

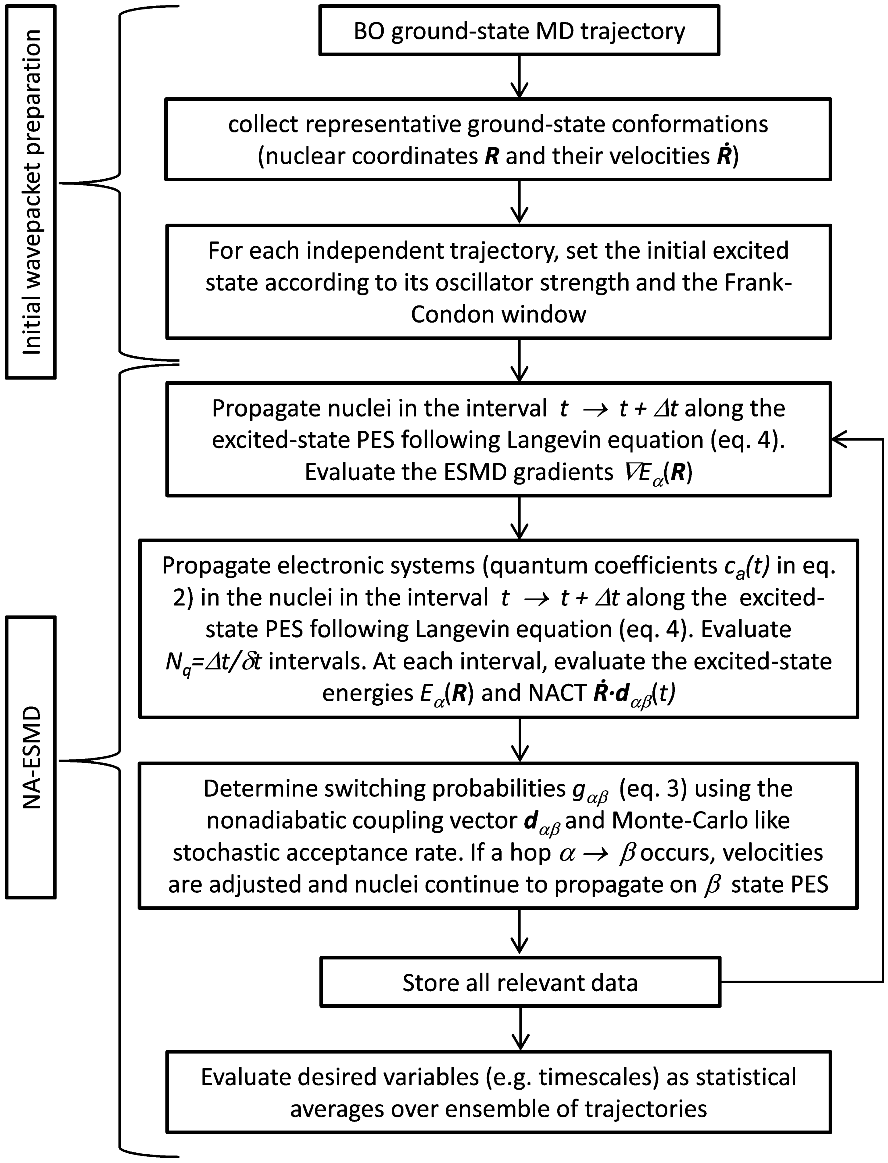

diagonal terms provide the occupation probabilities of adiabatic states.

The probability of hopping from the current state α to another state during the time interval Δt is related to the probability flux $\dot{a}_{\alpha\alpha}(t) = \sum_{\beta\neq\alpha} b_{\alpha\beta}$ (see eq 5 in section 2.3) where $b_{\beta\alpha}(t) = -2\mathrm{Re}(a^{*}_{\alpha\beta}\dot{\mathbf{R}}\cdot\mathbf{d}_{\alpha\beta})$[18] and hops are accepted or rejected stochastically.[26] Following a hop, nuclei evolve on the PES of the new state, and energy is conserved by rescaling nuclear velocities along the direction of NACR.[41] If the nuclear kinetic energy is insufficient to allow a hop to higher energy, then the hop is *classically forbidden* and is rejected.

2.2. Initial Wavepacket Preparation

NA-ESMD requires an ensemble of classical trajectories. The initial conformational sampling should represent the equilibrated ensemble at given thermodynamic conditions and provide statistical convergence of results. This requires computing a long ground-state BO trajectory from which a set of initial geometries $\mathbf{R}$ and nuclear velocities $\dot{\mathbf{R}}$ are collected. Compared with reference NA-ESMD simulations of a poly(phenylene vinylene) trimer following a 4.5 eV excitation using 1080 trajectories, ~400 trajectories generally provide statistically converged results with less than 5% error.[27]

For each trajectory, the initial excited state is chosen according to a Gaussian shaped Franck–Condon window[42]

$$\chi_{\alpha}(\mathbf{r};\,\mathbf{R}) = \exp[-T^2(E_{\mathrm{laser}} - \Omega_{\alpha})^2] \tag{3}$$

where E_{laser} represents the laser energy, Ω_{α} represents the energy of state α, and T is related to the full width at half-maximum as fwhm = $2(2\ \ln 2)^{1/2}T$. Oscillator strengths computed for each state are weighted by $\chi_{\alpha}(\mathbf{r};\,\mathbf{R})$, and the initial state is chosen by comparing the weighted value with a random number.

2.3. Nuclear and Electronic Propagation

Nuclei evolve along the excited-state PES according to constant temperature Langevin dynamics,

$$M_i\ddot{R}_i(t) = -\nabla E_{\alpha}(\mathbf{R}(t)) - \gamma M_i\dot{R}_i(t) + \mathbf{A}(t) \tag{4}$$

dx.doi.org/10.1021/ar400263p | *Acc. Chem. Res.* 2014, 47, 1155–1164

developed to be consistent with velocity Verlet integration.[43] M_i, $\ddot{R}_i$, and $\dot{R}_i$ give the mass, acceleration, and velocity, respectively, of the i^{th} nucleus. The stochastic force, **A**, depends on the bath temperature and the friction coefficient, γ (ps^{-1}). Excited-state energies, $E_\alpha(\mathbf{R})$, and gradients entering eq 2 are calculated at every trajectory point $\mathbf{R}(t)$ with time-step Δt for the nuclear propagation. Nuclear motion is governed by "native" excited-state gradients, $\nabla E_\alpha(\mathbf{R}(t))$, which are calculated analytically.[33,35,36] Utilization of state-specific forces promotes vibrational relaxation toward the excited-state optimal geometry in BO dynamics allowing the effects of differential nuclear motion to be seen. During NA dynamics, state-specific forces promote electronic and vibrational energy funneling to the lowest excited state (as seen in light harvesting dendrimers[44−46]). These findings discourage any attempt to address photodynamics in extended conjugated molecules using the classical-path approximation (CPA),[47] which assumes that ground-state nuclear dynamics can be used to study excited-state processes.

Fast electronic dynamics require a smaller quantum time-step $\delta t < \Delta t$ for propagating quantum coefficients. Excited-state energies and NACTs between all pairs of excited states are evaluated at each classical time-step and each intermediate δt. The value of δt must be sufficiently small to resolve strongly localized NACT peaks; otherwise transition probabilities can be underestimated.[27] Electronic coefficients are propagated according to eq 2 and switching probabilities, $g_{\alpha\beta}$, are evaluated at each classical step as a summation over all N_q quantum steps per classical step ($N_q = \Delta t/\delta t$)[41]

$$g_{\alpha\beta} = \frac{\sum_{j=1}^{N_q} b_{\beta\alpha}(j)\delta t}{a_{\alpha\alpha}} \tag{5}$$

2.4. Electronic Decoherence

The standard FSSH algorithm[18,41] propagates quantum coefficients coherently along each trajectory. In the single trajectory picture, classical treatment of nuclei does not provide any mechanism for dissipating electronic coherence.[48] This results in internal inconsistency characterized by a disagreement between the fraction of classical trajectories evolving on a given state and the average quantum population for that state. Because of that, various methods designed to incorporate decoherence in MDQT simulations have been developed.[49−54] We adopt the *instantaneous decoherence* approach, performed by resetting the quantum amplitude of the current state to unity after every attempted hop (regardless of whether hops are allowed or forbidden). This simple method is based on the assumption that wavepackets traveling on different surfaces should immediately separate in phase space and evolve independently. The approach provides qualitative improvement in the agreement between classical and quantum systems[29] at no additional computational cost and should also allow the coherent nature of transfer dynamics on ultrafast time scales to be captured; however this requires further study.

2.5. Transition Density Analysis

The evolution of adiabatic wave functions can be tracked by following changes in the spatial localization of the transition density (TD) of the current state. Diagonal elements of TD matrices $(\rho^{g\alpha})_{nn} \equiv \langle \phi_\alpha(t)|c_n^+ c_n|\phi_g(t)\rangle$ represent the net change in the electronic density distribution induced on an atomic orbital when undergoing a ground to excited state transition. These are computed using the CEO approach[30,31] where c_n^+ (c_n) are creation (annihilation) operators and $\phi_g(t)$ and $\phi_\alpha(t)$ are the ground- and excited-state CIS adiabatic wave functions, respectively. The fraction of TD localized on a molecular fragment is simply the sum of atomic contributions.[40] In this way, TD analysis allows the evolution of the electronic wave function to be followed providing a simplified picture of dynamics that does not rely on adiabatic state populations.[28,42,55]

2.6. Detection of Trivial Unavoided Crossings

Unavoided PES crossings are common events during radiationless vibronic[56] relaxation, and they have significant effects on photochemistry.[56,57] For small- and medium-sized conjugated molecules, unavoided crossings take place between interacting states that temporarily become coupled. In extended polyatomic molecules composed of weakly coupled chromophore units, special cases of unavoided crossings can occur between two noninteracting states localized on spatially separated moieties. In such cases, denoted as *trivial unavoided crossings*, NACTs behave as sharp peaks strongly localized at the exact crossing point, while they vanish elsewhere. This introduces a technical problem in "on-the-fly" surface hopping simulations: the use of finite time step numerical propagators for nuclear motion can cause such crossing points to be missed. Failure to detect these crossings will cause adiabatic states, defined according to their energy ordering, to be misidentified leading to artifacts in adiabatic state populations.[28,58]

To address this issue, we have developed an algorithm (described in detail in ref 28) to identify unavoided crossings by tracking state identities over time. This allows unavoided crossings involving interacting states (simulated by quantum hops) and trivial unavoided crossings between noninteracting states (detected by state tracking) to be distinguished from one another. The correspondence between new states at the current time-step i and old states at $(i - 1)$ is found based on the highest values of their overlaps. Maximization of the trace of the square of the overlap matrix, **S**, with elements defined as[28]

$$\begin{aligned} s_{\alpha\beta}(t;\, t + \Delta t) &\equiv \phi_\beta(\mathbf{r};\, \mathbf{R}(t)) \cdot \phi_\alpha(\mathbf{r};\, \mathbf{R}(t + \Delta t)) \\ &= \sum_{n,m} \rho^{g\beta}(t)_{nm} \rho^{g\alpha}(t + \Delta t)_{mn} \end{aligned} \tag{6}$$

is done using a Min-Cost algorithm. If a maximum overlap greater than an arbitrary threshold is identified, then the states are reassigned; their populations are interchanged, their couplings are canceled, and the hopping probability is not evaluated.

3. CONFORMATIONAL DYNAMICS IN POLYFLUORENES

NA-ESMD has been applied to study ultrafast conformational dynamics of conjugated polyfluorenes.[59] The model pentamer is shown in Figure 2A where the ground-state optimal geometry has significant distortion, ∼40° torsional angle between neighboring units. Pump−probe spectroscopy of polyfluorenes revealed fascinating ultrafast (60 fs) relaxation of the highly excited state, S_n, back to the lowest energy excited state, S_1 (see Figure 2B for schematic of relevant states). This rivals rhodopsin photoisomerization time scales, one of the fastest conformational processes in nature.[60] Experimental data[59] indicates that ultrafast photoinduced relaxation is accompanied by planarization of the polymer. We have used NA-ESMD calculations to reproduce and rationalize experimental findings by modeling relaxation from the different excited states (S_n and S_m) of polyfluorene. S_1 and S_m are one-photon transitions, while S_n requires two photons

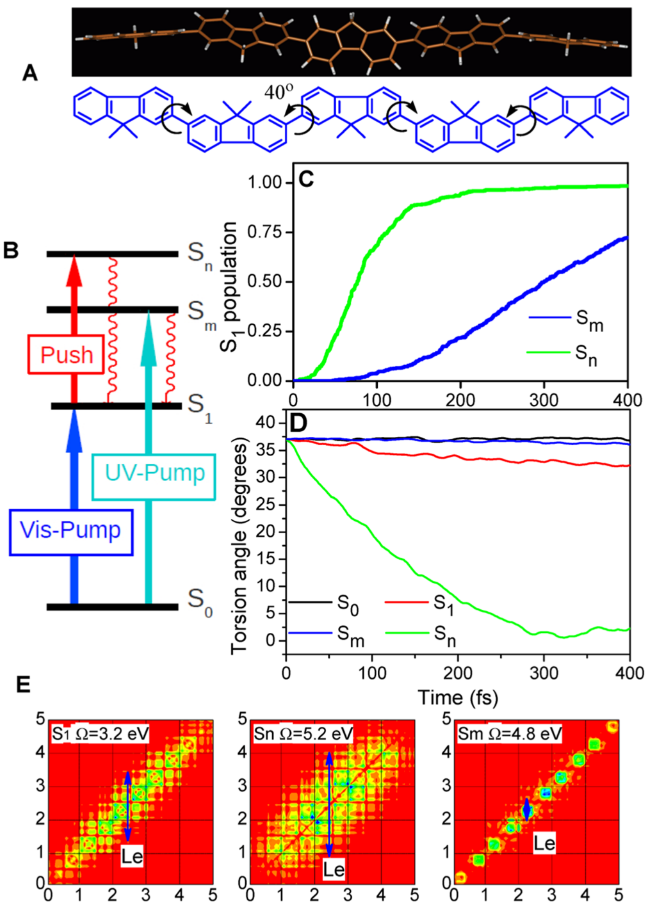

Figure 2. (A) Chemical structure of polyfluorene pentamer and MD snapshot showing twisted configuration. (B) Schematic of S_0, S_1, S_m, and S_n states. (C) S_1 population during NA-ESMD simulations starting from S_m (blue) and S_n (green). (D) Average variation of the minimum torsion angle between fluorene units during dynamics for S_0 (black), S_1 (red), S_m (blue), and S_n (green) states. (E) Transition density matrix plots of S_1, S_n, and S_m for the polyfluorene pentamer. Axes label the repeat oligomer units. Each plot depicts probabilities of an electron moving from one position (horizontal axis) to another (vertical axis) following excitation and Le defines the exciton size. Detailed results are reported in ref 59.

(sequential pump + push). After populating the S_n (or S_m) state of the pentamer, 500 NA-ESMD trajectories were propagated. BO dynamics of the ground-state, S_0, and the first excited state, S_1, were simulated as a reference.

Figure 2C shows the S_1 population as a function of time (computed as the fraction of trajectories in S_1) revealing that the photoexcited wavepacket placed in S_n undergoes internal conversion ($S_n \rightarrow S_1$) within 100 fs. However, internal conversion from the S_m state is much slower (∼500 fs). Figure 2D shows that the ultrafast internal conversion from S_n is accompanied by a local flattening of the molecule, whereas the dihedral angles do not change substantially during relaxation from other states. The CEO analysis of participating excited states (Figure 2E) identifies S_1 as a strongly bound exciton state corresponding to the lowest band gap transition. The S_n state is a delocalized transition with weak electron−hole interaction due to their large spatial separation of about three repeat units. Finally, the S_m state is a localized transition where an electron and hole are confined to a single phenyl ring.

The ultrafast internal conversion is aided by many factors. First, the underlying NA dynamics involve transitions between the ∼50 intermediate states occupying the 1.6 eV gap between S_n and S_1. These dense intermediate states form a continuum with no gaps, and similar to S_n, they are delocalized[61] resulting in large NACTs and promoting fast down-energy transitions. Second, PESs of delocalized excitons are relatively steep along the torsional degree of freedom and along the high-frequency C=C stretching motions. Consequently, the wavepacket gains substantial velocity along these two strongly coupled vibrational coordinates, transferring excess electronic energy into vibrations. In particular, owing to the many NA transitions between S_n and S_1 states, momentum is donated to torsional motion causing nuclei to gain such high kinetic energy that rapid planarization occurs within 100 fs. Relaxation from the S_m state cannot use the same efficient pathway followed by S_n owing to reduced NA coupling between localized (S_m) and delocalized intermediate states. As a result, the internal conversion from S_m is much slower. This observed ultrafast torsional relaxation may be exploited for nonlinear optical processes in organic systems and optical switching.

4. CONFORMATIONAL DISORDER AND ENERGY TRANSFER IN PHENYLENE VINYLENES

We have used NA-ESMD to investigate the effect of conformational disorder in energy transfer between two poly(phenylene

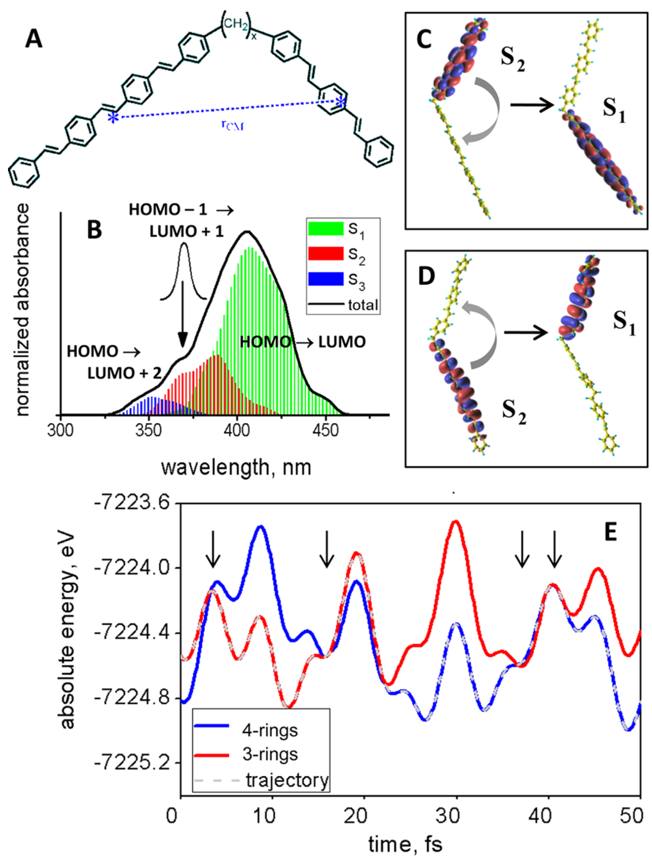

Figure 3. (A) Chemical structure of PPV oligomers. (B) Simulated absorbance spectrum and dominant orbital level excitations for the system separated by 19.5 Å. (C) Three-ring → four-ring pathway from the equilibrium geometry and (D) four-ring → three-ring pathway from a twisted geometry. (E) Potential energy of the two lowest energy states during the first 50 fs of dynamics. The red state is localized on the three-ring fragment, the blue state is localized on the four-ring fragment, and dashes show the trajectory path. Multiple trivial unavoided crossings occur as indicated by arrows. Detailed results are reported in ref 55.

dx.doi.org/10.1021/ar400263p | Acc. Chem. Res. 2014, 47, 1155−1164

vinylene) (PPV) fragments.[55] Linear polymer segments act as weakly coupled chromophore units that localize excitons. Following excitation, energy is transferred nonradiatively between segments.[62] However, linear segments have overlapping absorption meaning that fragments can act as both donors and acceptors. In addition, large dihedral angles between subunits can break conjugation[62] leading to changes in exciton localization. These unique features give rise to rich energy transfer dynamics involving multiple pathways. Recent studies suggest that electronic coherence plays an important role in energy transfer in PPV type polymers on ultrafast time scales.[63] These findings stress the importance of treating electronic decoherence (see section 2.4). The model system shown in Figure 3A is composed of three- and four-ring PPV segments separated by varying distances. The total absorption spectrum for segments separated by 19.5 Å (Figure 3B) can be interpreted as the sum of contributions from each fragment with strong overlap. For the equilibrium geometry, the lowest energy excited state S_1 (HOMO → LUMO; hereafter only dominating orbital excitation is indicated) is localized on the four-ring segment, S_2 (HOMO − 1 → LUMO + 1) is localized on the three-ring segment, and S_3 (HOMO → LUMO + 2) is localized on the four-ring segment. Excitation at 370 nm maximizes absorption by S_2 but cannot exclude the overlapping S_3 state.

The initial localization depends on the initial state and configuration. For example, Figure 3C shows that following excitation to S_2, the TD primarily localized on the three-ring segment is transferred to the four-ring segment as the system relaxes to S_1, consistent with the equilibrium geometry localization. However, the twisted configuration in Figure 3D causes reordering of excited-state energies: S_2 becomes localized on the four-ring segment, while S_1 is localized on the three-ring segment, and energy transfer proceeds in the reverse four-ring → three-ring direction. When S_3 serves as the initial state, the state localized on the three-ring segment can act as an intermediate in a three-state process where transient energy transfer occurs. The picture is further complicated by fluctuations in the dihedral angles between subunits causing multiple state crossings and near degeneracies during dynamics. This can be seen in Figure 3E for a single representative trajectory; energy transfer becomes unlikely after the first trivial unavoided crossing because it requires an upward energy transition. In this way, energy transfer

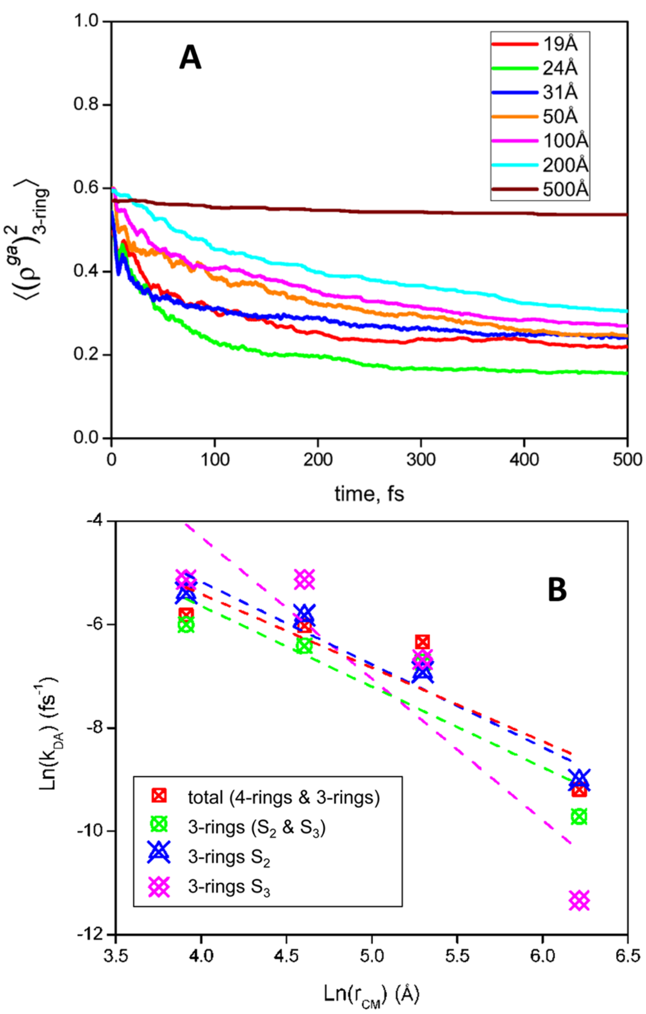

Figure 4. (A) Decay of the transition density localized in the three-ring fragment for each separation distance reveals energy transfer. (B) NA-EMSD energy transfer rates as a function of separation distance for different pathways. Detailed results are reported in ref 55.

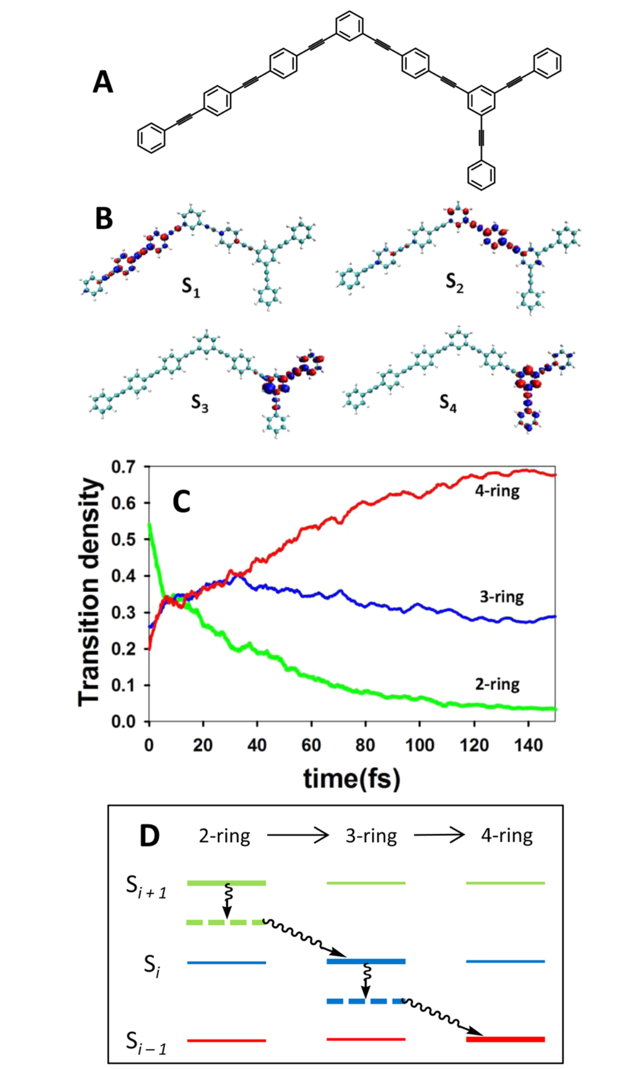

Figure 5. (A) Chemical structure of the model PPE branched oligomer. (B) Initial localization of transition densities for states S_1–S_4. (C) Evolution of the transition density localized in each segment during NA-ESMD simulations. (D) Schematic of the *shishiodoshi* unidirectional energy transfer mechanism. Detailed results are reported in ref 42.

dx.doi.org/10.1021/ar400263p | *Acc. Chem. Res.* 2014, 47, 1155−1164

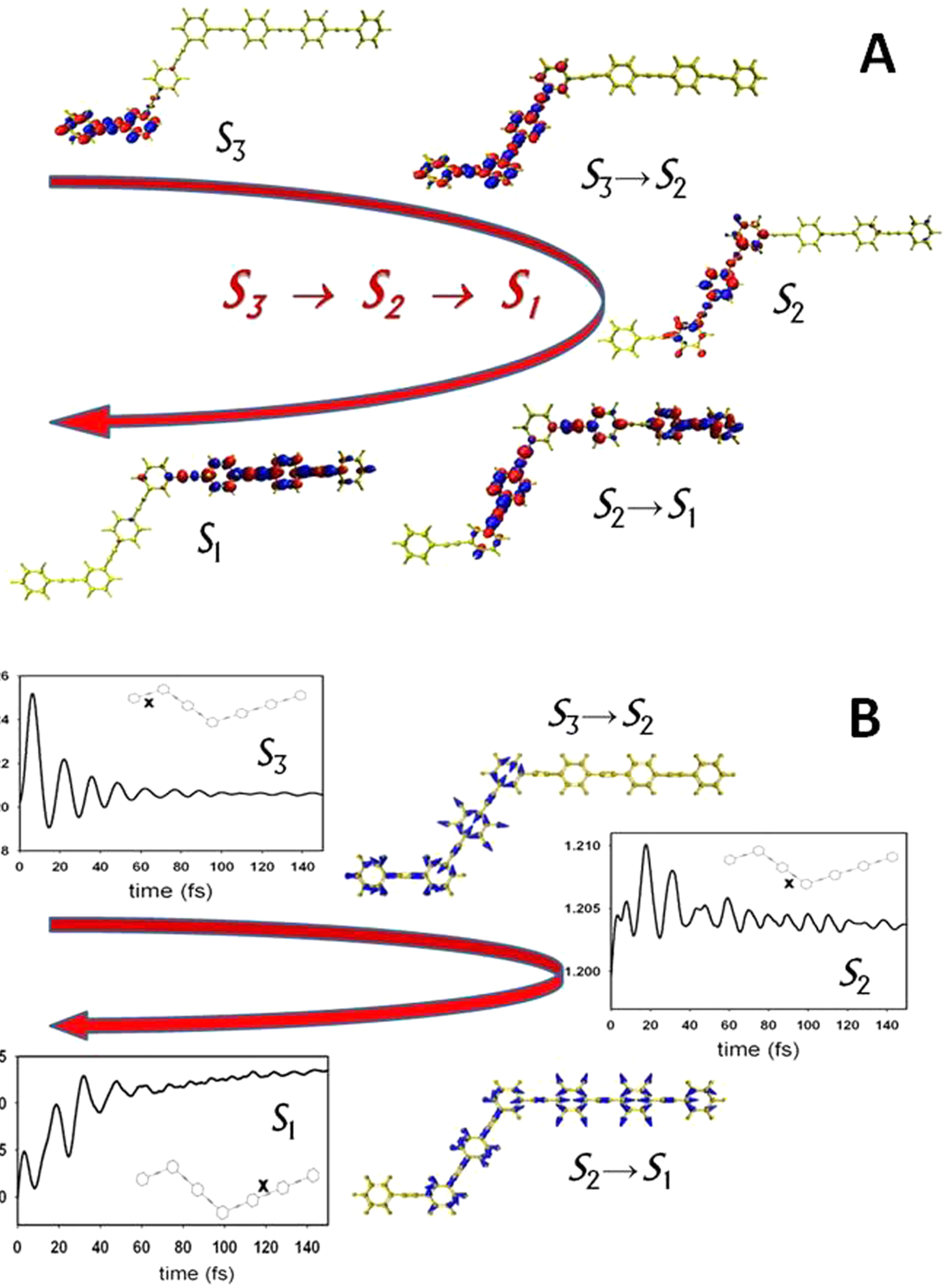

Figure 6. (A) Unidirectional two-ring → three-ring → four-ring energy transfer revealed by the transition density localization in PPE chromophores. (B) The C≡C stretching motion of each segment corresponds to the energy transfer. Analysis of state-specific vibrations reveals excited-state normal modes responsible for energy transfer and vibrational relaxation. Detailed results are reported in refs 45 and 46.

is linked to conformational fluctuations and is delayed until the original energy ordering is restored.

The energy transfer can be seen by following the decay of TD localized in the three-ring segment as shown in Figure 4A. Energy transfer rates were calculated for each separation distance by fitting the TD curves to a biexponential decay function. The dependence of the rate on the separation distance, r, is shown in Figure 4B for different pathways. The scaling of the NA-ESMD rates range from $1/r^2$ to $1/r^{3.9}$ for different pathways. However, due to the convolution of many competing energy transfer pathways, there is no agreement with the $1/r^6$ scaling predicted from Förster theory.[64] The added complexity of conformational disorder leading to repeated instances of excited-state energy reordering makes it impossible to describe energy transfer in soft polymer systems using a single-rate description.

5. UNIDIRECTIONAL ENERGY TRANSFER IN DENDRIMERS

The highly efficient intramolecular energy transfer in poly-(phenylene ethynylene) (PPE) dendrimers has been the subject of several theoretical and experimental studies.[65−67] NA-ESMD has been used to investigate the mechanism leading to this highly efficient ultrafast energy transfer.[42,44−46] The model system, depicted in Figure 5A, is composed of two-, three-, and four-ring linear PPE chromophores linked by meta-substitutions representing building blocks similar to those comprising the well-known "nanostar" dendrimer.[68,69] As shown in Figure 5B, meta-branching localizes excitations within each fragment. Dendrimers of these building blocks have been shown to undergo highly efficient and unidirectional electronic and vibrational energy transfer.

NA-ESMD simulations of the model system depicted in Figure 5A were performed after excitation to the state primarily localized in the two-ring units. The energy transfer can be followed as the time-dependent fraction of TD localized in each unit as shown in Figure 5C. TD is initially localized in the two-ring unit, but within 80−100 fs an almost complete ultrafast electronic energy transfer to the three- and four-ring units takes place. Through-space (two-ring → four-ring) and sequential through-bond (two-ring → three-ring → four-ring) energy transfer mechanisms are expected to exist in competition with one another. The transient increase in TD localized in the three-ring unit suggests that this unit acts as a bridge.

We have identified features that lead to efficient unidirectional energy transfer. The schematic in Figure 5D outlines the *shishiodoshi* unidirectional energy transfer mechanism: while the electronic population is mostly in states localized in the two-ring units, the nuclear motion keeps the current state S_{i+1} close in energy to the state immediately below, thus favoring the energy transfer between S_{i+1} and S_i. Once the electronic population has been significantly transferred to states localized on the three-ring unit, the nuclear motion on the new surface decouples the old states while coupling the new state S_i with the state below S_{i-1}. The coupling between these new states persists until most of the population has been transferred to the state localized in the four-ring unit. This guarantees an efficient unidirectional two-ring → three-ring → four-ring energy flow.

Finally, we confirm that the electronic energy transfer shown in Figure 6A for a related PPE dendrimer is concomitant with vibrational energy transfer through a dominant C≡C stretching motion shown in Figure 6B. Our analysis of the state-specific vibrations during NA transitions allows the identification of excited-state normal modes that act as "bridges" through which efficient energy funneling occurs.[45] The photoinduced energy transfer represents a concerted electronic and vibrational process. The observed mechanism highlights the importance of using native excited-state forces in order to capture the effect of differential nuclear motion.

6. CONCLUSION

Until recently, FSSH has been successfully applied to systems involving only a few excited states, and it has been unclear whether the generalized framework developed and tested for small systems can be applied to larger polyatomic systems involving many excited states and multiple unavoided PES crossings. The necessity of propagating a large ensemble of trajectories rules out any practical application of sophisticated excited-state *ab initio* methodologies to extended molecular systems with large densities of excited states participating in photoinduced dynamics. The NA-ESMD framework described above provides a computationally efficient and accurate description of photoinduced dynamics in extended conjugated molecular systems. These advantages have opened the door to study new systems, largely inaccessible to previous methods, consisting of hundreds of atoms on time-scales of tens of picoseconds. Nonadiabatic dynamics simulations not only agree with experiment but are capable of providing detailed insights into the mechanisms responsible for complex photoinduced processes. As the field progresses toward ever increasing predictive power, it is essential to have advanced theoretical capabilities at our disposal. In this respect, NA-ESMD is a continually evolving tool capable of treating the growing complexity of technologically and biologically relevant systems.

AUTHOR INFORMATION

Funding

This work was supported by CONICET, UNQ, ANPCyT (Grant PICT-2010-2375), National Science Foundation Grant Nos. CHE-0239129 and CHE-0808910, and U.S. Department of Energy and Los Alamos LDRD funds. Los Alamos National Laboratory is operated by Los Alamos National Security, LLC, for the National Nuclear Security Administration of the U.S. Department of Energy under Contract DE-AC5206NA25396. We acknowledge support from the Center for Integrated Nanotechnologies (CINT) and the Center for Nonlinear Studies (CNLS) at LANL.

Notes

The authors declare no competing financial interest.

Biographies

Tammie Nelson received her undergraduate degree from California Polytechnic State University in San Luis Obispo in 2008 and her Ph.D. in Chemistry from University of Rochester, NY, in 2013. She is currently director's funded postdoctoral fellow at Los Alamos National Laboratory. Her research has focused on modeling nonadiabatic dynamics and photoinduced processes in extended molecular systems.

Sebastian Fernandez-Alberti is currently a Full Professor at National University of Quilmes (UNQ, Argentina) and Independent Researcher at the National Council for Scientific and Technical Research (CONICET, Argentina). He received his degree in 1993 from the National University of La Plata (UNLP, Argentina) and his Ph.D. in Molecular Physics in 1999 from the University of Paul Sabatier (Toulouse, France). His research interests include nonadiabatic dynamics, vibrational relaxation, and intramolecular energy redistribution in polyatomic molecules, and protein dynamics.

Adrian E. Roitberg obtained his undergraduate degree from the University of Buenos Aires in Argentina and his Ph.D. from the University of Illinois at Chicago in 1992. He performed postdoctoral studies at Northwestern University and joined NIST in 1995. Since 2001, he has been Professor of Chemistry and Physics at the University of Florida. His research emphasizes the application of molecular dynamics tools to biological systems as well as excited state dynamics in polymers.

Sergei Tretiak is a Staff Scientist at Los Alamos National Laboratory and the Center for Integrated Nanotechnologies (CINT). He received his M.Sc. (1994) from Moscow Institute of Physics and Technology (Russia) and his Ph.D. (1998) from the University of Rochester, NY, where he worked with Prof. Shaul Mukamel. His research interests include developing computational methods for optical properties in nanoscale materials, nonadiabatic molecular dynamics of excited states, and charge and energy transfer in biological and artificial antenna complexes.

REFERENCES

(1) Satishkumar, B. C.; Brown, L. O.; Gao, Y.; Wang, C. C.; Wang, H. L.; Doorn, S. K. Reversible fluorescence quenching in carbon nanotubes for biomolecular sensing. *Nat. Nanotechnol.* **2007**, *2*, 560−564.

(2) Granstrom, M.; Petritsch, K.; Arias, A. C.; Lux, A.; Andersson, M. R.; Friend, R. H. Laminated fabrication of polymeric photovoltaic diodes. *Nature* **1998**, *395*, 257−260.

(3) Cao, Y.; Parker, I. D.; Yu, G.; Zhang, C.; Heeger, A. J. Improved quantum efficiency for electroluminescence in semiconducting polymers. *Nature* **1999**, *397*, 414−417.

(4) Bredas, J. L.; Norton, J. E.; Cornil, J.; Coropceanu, V. Molecular understanding of organic solar cells: The challenges. *Acc. Chem. Res.* **2009**, *42*, 1691−1699.

(5) Sirringhaus, H.; Kawase, T.; Friend, R. H.; Shimoda, T.; Inbasekaran, M.; Wu, W.; Woo, E. P. High-resolution inkjet printing of all-polymer transistor circuits. *Science* **2000**, *290*, 2123−2126.

(6) Friend, R. H.; Gymer, R. W.; Holmes, A. B.; Burroughes, J. H.; Marks, R. N.; Taliani, C.; Bradley, D. D. C.; dos Santos, D. A.; Bredas, J. L.; Logdlund, M.; Salaneck, W. R. Electroluminescence in conjugated polymers. *Nature* **1999**, *397*, 121−128.

(7) Tretiak, S.; Saxena, A.; Martin, R. L.; Bishop, A. R. Conformational dynamics of photoexcited conjugated molecules. *Phys. Rev. Lett.* **2002**, *89*, No. 097402.

(8) Olivucci, M. *Computational Photochemistry*; Elsevier: Amsterdam, 2005.

(9) Niklasson, A. M.; Steneteg, P.; Odell, A.; Bock, N.; Challacombe, M.; Tymczak, C. J.; Holmström, E.; Zheng, G.; Weber, V. Extended Langevin Born-Oppenheimer molecular dynamics with dissipation. *J. Chem. Phys.* **2009**, *130*, No. 214109.

(10) Karabunarliev, S.; Baumgarten, M.; Müllen, K. Adiabatic one- and two-photon excited states in phenylene-based conjugated oligomers: A quantum-chemical study. *J. Phys. Chem. A* **2000**, *104*, 8236−8243.

(11) Molnar, F.; Ben-Nun, M.; Martinez, T. J.; Schulten, K. Characterization of conical intersections between the ground and first excited state for a retinal analog. *J. Mol. Struct. Theochem.* **2000**, *506*, 169−178.

(12) Franco, I.; Tretiak, S. Electron-vibrational dynamics of photoexcited polyfluorenes. *J. Am. Chem. Soc.* **2004**, *126*, 12130−12140.

(13) Gambetta, A.; Manzoni, C.; Menna, E.; Meneghetti, M.; Cerullo, G.; Lanzani, G.; Tretiak, S.; Piryatinski, A.; Saxena, A.; Martin, R. L.; Bishop, A. R. Real-time observation of nonlinear coherent phonon dynamics in single-walled carbon nanotubes. *Nat. Phys.* **2006**, *2*, 515−520.

(14) Jasper, A. W.; Nangia, S.; Zhu, C.; Truhlar, D. G. Non-Born−Oppenheimer molecular dynamics. *Acc. Chem. Res.* **2006**, *39*, 101−108.

(15) Martinez, T. J. Insights for light-driven molecular devices from ab initio multiple spawning excited-state dynamics of organic and biological chromophores. *Acc. Chem. Res.* **2006**, *39*, 119−126.

(16) Worth, G. A.; Meyer, H.-D.; Köppel, H.; Cederbaum, L. S.; Burghardt, I. Using the MCTDH wavepacket propagation method to describe multimode non-adiabatic dynamics. *Int. Rev. Phys. Chem.* **2008**, *27*, 569−606.

(17) Tamura, H.; Burghardt, I. Ultrafast charge separation in organic photovoltaics enhanced by charge delocalization and vibronically hot exciton dissociation. *J. Am. Chem. Soc.* **2013**, *135*, 16364−16367.

(18) Tully, J. C. Molecular dynamics with electronic transitions. *J. Chem. Phys.* **1990**, *93*, 1061−1071.

(19) Hack, M. D.; Jasper, A. W.; Volobuev, Y. L.; Schwenke, D. W.; Truhlar, D. G. Quantum mechanical and quasiclassical trajectory surface hopping studies of the electronically nonadiabatic predissociation of the A state in NaH_2. *J. Phys. Chem. A* **1999**, *103*, 6309−6326.

(20) Fernandez-Alberti, S.; Halberstadt, N.; Beswick, J. A.; Echave, J. A theoretical study of photofragmentation and geminate recombination of ICN in solid Ar. *J. Chem. Phys.* **1998**, *109*, 2844−2850.

(21) Hammes-Schiffer, S. Hydrogen tunneling and protein motion in enzyme reactions. *Acc. Chem. Res.* **2006**, *39*, 93−100.

(22) Antol, I.; Eckert-Maksic, M.; Barbatti, M.; Lischka, H. Simulation of the photodeactivation of formamide in the n_O-π^* and π−π^* states: An *ab initio* on-the-fly surface-hopping dynamic study. *J. Chem. Phys.* **2007**, *127*, No. 234303.

(23) Prezhdo, O. V. Photoinduced dynamics in semiconductor quantum dots: insights from time-domain ab initio studies. *Acc. Chem. Res.* **2009**, *42*, 2005−2016.

(24) Neukirch, A. J.; Shamberger, L. C.; Abad, E.; Haycock, B. J.; Wang, H.; Ortega, J.; Prezhdo, O. V.; Lewis, J. P. Nonadiabatic ensemble simulations of cis-stilbene and cis-azobenzene photoisomerization. *J. Chem. Theory Comput.* **2014**, *10*, 14−23.

(25) Subotnik, J. E.; Shenvi, N. A new approach to decoherence and momentum rescaling in the surface hopping algorithm. *J. Chem. Phys.* **2011**, *134*, No. 024105.

(26) Nelson, T.; Fernandez-Alberti, S.; Chernyak, V.; Roitberg, A. E.; Tretiak, S. Nonadiabatic excited state molecular dynamics modeling of photoinduced dynamics in conjugated molecules. *J. Phys. Chem. B* **2011**, *115*, 5402−5414.

(27) Nelson, T.; Fernandez-Alberti, S.; Chernyak, V.; Roitberg, A. E.; Tretiak, S. Nonadiabatic excited state molecular dynamics: numerical tests of convergence and parameters. *J. Chem. Phys.* **2012**, *136*, No. 054108.

(28) Fernandez-Alberti, S.; Roitberg, A. E.; Nelson, T.; Tretiak, S. Identification of unavoided crossings in nonadiabatic photoexcited dynamics involving multiple electronic states in polyatomic conjugated molecules. *J. Chem. Phys.* **2012**, *137*, No. 014512.

(29) Nelson, T.; Fernandez-Alberti, S.; Roitberg, A. E.; Tretiak, S. Nonadiabatic excited state molecular dynamics: Treatment of electronic decoherence. *J. Chem. Phys.* **2013**, *138*, No. 224111.

(30) Tretiak, S.; Mukamel, S. Density matrix analysis and simulation of electronic excitations in conjugated and aggregated molecules. *Chem. Rev.* **2002**, *102*, 3171−3212.

(31) Mukamel, S.; Tretiak, S.; Wagersreiter, T.; Chernyak, V. Electronic coherence and collective optical excitations of conjugated molecules. *Science* **1997**, *277*, 781−787.

(32) Thouless, D. J. *The Quantum Mechanics of Many-Body Systems*; Academic Press: New York, 1972.

(33) Dewar, M. J. S.; Zoebisch, E. G.; Healy, E. F.; Stewart, J. J. P. AM1: A new general purpose quantum mechanical molecular model. *J. Am. Chem. Soc.* **1985**, *107*, 3902−3909.

(34) Dreuw, A.; Head-Gordon, M. Single-reference ab initio methods for the calculation of excited states of large molecules. *Chem. Rev.* **2005**, *105*, 4009−4037.

(35) Furche, F. On the density matrix based approach to time-dependent density functional response theory. *J. Chem. Phys.* **2001**, *114*, 5982−5992.

(36) Furche, F.; Ahlrichs, R. Adiabatic time-dependent density functional methods for excited state properties. *J. Chem. Phys.* **2002**, *117*, 7433−7447.

(37) Tretiak, S.; Chernyak, V. Resonant nonlinear polarizabilities in the time-dependent functional theory. *J. Chem. Phys.* **2003**, *119*, 8809−8823.

(38) Chernyak, V.; Mukamel, S. Density-matrix representation of nonadiabatic couplings in time-dependent density functional (TDDFT) theories. *J. Chem. Phys.* **2000**, *112*, 3572−3579.

(39) Tommasini, M.; Chernyak, V.; Mukamel, S. Electronic density-matrix algorithm for nonadiabatic couplings in molecular dynamics simulations. *Int. J. Quantum Chem.* **2001**, *85*, 225−238.

(40) Baer, M. *Beyond Born Oppenheimer: Electronic Non-Adiabatic Coupling Terms and Conical Intersections*; Wiley: Hoboken, NJ, 2006.

(41) Hammes-Schiffer, S.; Tully, J. C. Proton transfer in solution: Molecular dynamics with quantum transitions. *J. Chem. Phys.* **1994**, *101*, 4657−4667.

(42) Fernandez-Alberti, S.; Roitberg, A. E.; Kleiman, V. D.; Nelson, T.; Tretiak, S. Shishiodoshi unidirectional energy transfer mechanism in phenylene ethynylene dendrimers. *J. Chem. Phys.* **2012**, *137*, No. 22A526.

(43) Paterlini, M. G.; Ferguson, D. M. Constant temperature simulations using the Langevin equation with velocity Verlet integration. *Chem. Phys.* **1998**, *236*, 243−252.

(44) Fernandez-Alberti, S.; Kleiman, V. D.; Tretiak, S.; Roitberg, A. E. Nonadiabatic molecular dynamics simulations of the energy transfer between building blocks in a phenylene ethynylene dendrimer. *J. Phys. Chem. A* **2009**, *113*, 7535−7542.

(45) Fernandez-Alberti, S.; Kleiman, V. D.; Tretiak, S.; Roitberg, A. E. Unidirectional energy transfer in conjugated molecules: the crucial role of high frequency C(triple)C bonds. *J. Phys. Chem. Lett.* **2010**, *1*, 2699−2704.

(46) Soler, M. A.; Roitberg, A. E.; Nelson, T.; Tretiak, S.; Fernandez-Alberti, S. Analysis of state-specific vibrations coupled to the unidirectional energy transfer in conjugated dendrimers. *J. Phys. Chem. A* **2012**, *116*, 9802−9810.
(47) Billing, G. D. Classical path method in inelastic and reactive scattering. *Int. Rev. Phys. Chem.* **1994**, *13*, 309.
(48) Tully, J. C. Perspective: Nonadiabatic dynamics theory. *J. Chem. Phys.* **2012**, *137*, No. 22A301.
(49) Bittner, E. R.; Rossky, P. J. Quantum decoherence in mixed quantum-classical systems: nonadiabatic processes. *J. Chem. Phys.* **1995**, *103*, 8130−8143.
(50) Subotnik, J. E.; Shenvi, N. A new approach to decoherence and momentum rescaling in the surface hopping algorithm. *J. Chem. Phys.* **2011**, *134*, No. 024105.
(51) Zhu, C.; Nangia, S.; Jasper, A. W.; Truhlar, D. G. Coherent switching with decay of mixing: An improved treatment of electronic coherence for non-Born-Oppenheimer trajectories. *J. Chem. Phys.* **2004**, *121*, 7658−7670.
(52) Granucci, G.; Persico, M. Critical appraisal of the fewest switches algorithm for surface hopping. *J. Chem. Phys.* **2007**, *126*, No. 134114.
(53) Jaeger, H. M.; Fischer, S.; Prezhdo, O. V. Decoherence-induced surface hopping. *J. Chem. Phys.* **2012**, *137*, No. 22A545.
(54) Gorshkov, V. N.; Tretiak, S.; Mozyrsky, D. Semiclassical Monte-Carlo approach for modeling non-adiabatic dynamics in extended molecules. *Nat. Commun.* **2013**, *4*, No. 2144.
(55) Nelson, T.; Fernandez-Alberti, S.; Roitberg, A. E.; Tretiak, S. Conformational disorder in energy transfer: beyond Forster theory. *Phys. Chem. Chem. Phys.* **2013**, *15*, 9245−9256.
(56) Domcke, W.; Yarkony, D. R. Role of conical intersections in molecular spectroscopy and photoinduced chemical dynamics. *Annu. Rev. Phys. Chem.* **2012**, *63*, 325−352.
(57) Mahapatra, S. Excited electronic states and nonadiabatic effects in contemporary chemical dynamics. *Acc. Chem. Res.* **2009**, *42*, 1004−1015.
(58) Nelson, T.; Fernandez-Alberti, S.; Roitberg, A. E.; Tretiak, S. Artifacts due to trivial unavoided crossings in the modeling of photoinduced energy transfer dynamics in extended conjugated molecules. *Chem. Phys. Lett.* **2013**, *590*, 208−213.
(59) Clark, J.; Nelson, T.; Tretiak, S.; Cirmi, G.; Lanzani, G. Femtosecond torsional relaxation. *Nat. Phys.* **2012**, *8*, 225−231.
(60) Shoenlein, R. W.; Peteanu, L. A.; Mathies, R. A.; Shank, C. V. The 1st step in vision − femtosecond isomerization of rhodopsin. *Science* **1991**, *254*, 412−415.
(61) Wu, C.; Malinin, S. V.; Tretiak, S.; Chernyak, V. Y. Exciton scattering and localization in branched dendrimeric structures. *Nat. Phys.* **2006**, *2*, 631−635.
(62) Bolinger, J.; Traub, M.; Brazard, J.; Adachi, T.; Barbara, P.; Bout, D. V. Conformation and energy transfer in single conjugated polymers. *Acc. Chem. Res.* **2012**, *45*, 1992−2001.
(63) Binder, R.; Wahl, J.; Romer, S.; Burghardt, I. Coherent exciton transport driven by torsional dynamics: a quantum dynamical study of phenylene-vinylene type conjugated systems. *Faraday Discuss.* **2013**, *163*, 205.
(64) Forster, T. *Ann. Phys.* **1948**, *437*, 55−75.
(65) Mukamel, S. Photochemistry: Trees to trap photons. *Nature* **1997**, *388*, 425−427.
(66) Swallen, S. F.; Zhu, Z.; Moore, J. S.; Kopelman, R. Correlated excimer formation and molecular rotational dynamics in phenyl-acetylene dendrimers. *J. Phys. Chem. B* **2000**, *104*, 3988−3995.
(67) Rana, D.; Gangopadhyay, G. Steady-state spectral properties of dendrimer supermolecule as a light harvesting system. *Chem. Phys. Lett.* **2001**, *334*, 314−324.
(68) Kopelman, R.; Shortreed, M.; Shi, Z.-Y.; Tan, W.; Moore, J. S.; Bar-Haim, A.; Klafter, J. Spectroscopic evidence for exciton localization in fractal antenna supermolecules. *Phys. Rev. Lett.* **1997**, *78*, 1239−1242.
(69) Devadoss, C.; Bharathi, P.; Moore, J. S. Energy transfer in dendritic macromolecules: molecular size effects and the role of an energy gradient. *J. Am. Chem. Soc.* **1996**, *118*, 9635−9644.